HENDRICKSON, W. A. & KONNERT, J. H. (1980). *Computing in Crystallography*, edited by R. Diamond, S. Ramaseshan & K. Venkatesan, pp. 13.01–13.23. Bangalore: Indian Academy of Sciences.

HOARD, L. G. & NORDMAN, C. E. (1979). *Acta Cryst.* **A35**, 1010–1015.

JACK, A. & LEVITT, M. (1978). *Acta Cryst.* **A34**, 931–935.

LESLIE, A. G. W. & WONACOTT, A. J. (1983). *J. Mol. Biol.* **165**, 375–391.

LESLIE, A. G. W. & WONACOTT, A. J. (1984). In preparation.

REMINGTON, S., WIEGAND, G. & HUBER, R. (1982). *J. Mol. Biol.* **158**, 111–152.

ROSSMANN, M. G. & BLOW, D. M. (1962). *Acta Cryst.* **15**, 24–31.

SCHERINGER, C. (1963). *Acta Cryst.* **16**, 546–550.

SMITH, P. J. C. & ARNOTT, S. (1978). *Acta Cryst.* **A34**, 3–11.

SUSSMAN, J. L., HOLBROOK, S. R., CHURCH, G. M. & KIM, S. H. (1977). *Acta Cryst.* **A33**, 800–804.

WONACOTT, A. J. (1983). Personal communication.

WONACOTT, A. J. & BIESECKER, G. (1977). In *Pyridine Nucleotide Dependent Dehydrogenases*, edited by H. SUND. Berlin, New York: Walter de Gruyter.

Acta Cryst. (1984). A**40**, 459–465

Investigation of a Silicon Single Crystal by Means of the Diffraction of Mössbauer Radiation

BY K. KREC AND W. STEINER

Institut für Angewandte und Technische Physik, Technische Universität Wien, Austria

(*Received* 30 *November* 1983; *accepted* 22 *February* 1984)

Abstract

Diffraction experiments with resonant γ-radiation were performed on a single crystal of silicon at room temperature. The high energy resolution of the Mössbauer effect was used to separate elastically and inelastically scattered radiation. A special experimental setup is described, which in addition allows the determination of the total thermal diffuse scattered intensity. Inelastically scattered radiation was observed in the whole investigated angular range. In the vicinity of Bragg reflections the ratio of the integrated intensities of inelastically to elastically scattered radiation was in very good agreement with the results of calculations using different computer programs based on first-order thermal diffuse scattering theory for a wide range of chosen scan lengths. The measured ratios of the elastically scattered radiation of different Bragg reflections were used to determine the temperature factor B.

I. Introduction

The precise determination of the thermal diffuse scattered (TDS) part of the diffracted radiation from a crystal is of great importance for the structure determination, since this contribution exhibits also a maximum value at the exact Bragg position and an error in the consideration of the integrated intensity can lead to an incorrect temperature factor B which may cause errors of the mean atomic coordinates or of the charge density due to the atomic scattering factors. In ordinary X-ray diffraction experiments an accurate determination of this TDS contribution is usually performed using theoretical models mainly based on the long-wavelength approximation. Several computer programs (Stevens, 1974; Helmholdt & Vos, 1977; Kurittu & Merisalo, 1977) are available which allow the calculation of integrated TDS intensities from the elastic constants taking into account the anisotropy of the elasticity. Experimentally the extraordinary high energy resolution of the Mössbauer effect can be used to separate elastically and inelastically scattered radiation from crystals not containing Mössbauer isotopes (O'Connor & Butt, 1963; Albanese, Ghezzi, Merlini & Pace, 1972; Albanese & Deriu, 1979) offering the possibility to test these theoretical calculations if special care is taken for the intensity measurements. In addition, the temperature factor B can be determined either directly from the elastically scattered intensities or with some assumptions concerning the TDS from the inelastically scattered intensities. Mössbauer diffraction on silicon was used to determine the reflecting power (Ghezzi, Merlini & Pace, 1969; Kashiwase & Minoura, 1983) and the dependence of the TDS intensities on both the reflecting angle and the temperature (Albanese *et al.*, 1972). Whereas the temperature and angle dependence of TDS is in good agreement with the prediction of the lattice wave theory (Warren, 1969), an evaluation of the fraction of the TDS intensities on the total intensities was not possible with reasonable accuracy (Ghezzi *et al.*, 1969) because (i) the quality of the crystals was not known with high accuracy and (ii) an experimental separation of the TDS contribution to the background could not be performed.

It is the aim of the present paper to show that several improvements of the experimental setup allow

0108-7673/84/040459-07$01.50

a very precise determination not only of the elastically and inelastically scattered radiation, but also of the TDS included in the background. Therefore an experimental test of the calculated TDS contributions is possible and in spite of the long measuring times caused by the low activity of Mössbauer sources, which limit the number of measured reflections, B can be evaluated, if the crystal quality is known. Silicon was selected since commercially single crystals with a high degree of perfection are available, which allow the application of the dynamical theory. Furthermore, the elastic constants which have to be used in the computer programs and the atomic scattering factors needed to calculate diffracting powers are known with high accuracy and recently Robertson & Reid (1979) and Reid & Pirie (1980) performed *ab initio* calculations of intensities of the total phonon scattering and Debye–Waller factors.

In § II a description of the experimental setup is given. The results for the elastically and inelastically scattered intensities are presented and discussed in comparison with theory in § III.

II. Experimental details

The general setup of a Mössbauer diffractometer is similar to that of an ordinary X-ray diffraction experiment with the exception that the X-ray tube has to be exchanged for a Mössbauer source (O'Connor & Butt, 1963; Albanese *et al.*, 1972). To obtain a rigid connection between the source [^{57}Co *Rh*, 100 mCi (1 Ci = 37 GBq)], the crystal and the resonant absorber (^{57}Fe *Rh*) and to avoid unwanted movements of source, crystal and absorber against each other a special two-circle goniometer was constructed (Fig. 1). The γ quanta passing through the absorber were counted by means of a Si(Li) detector with an energy resolution of 300 eV at 14.4 keV. The distance between source and crystal was 155 mm, that between crystal and counter 95 mm. The detector was fixed in position, the source and the crystal could be rotated. In addition, the crystal could be rotated about ± 15°

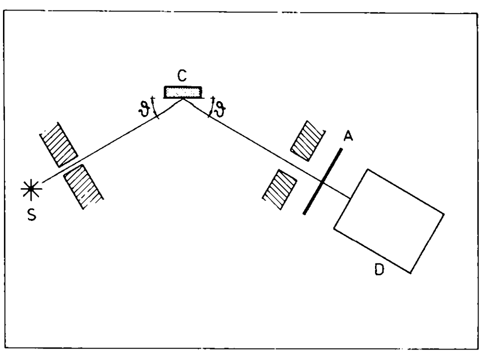

Fig. 1. Schematic drawing of the experimental setup. (S Mössbauer source, moved with different velocities, C crystal, A resonant absorber, D detector.)

in two vertical planes, perpendicular to each other. Thus, in a limited range an operation similar to that of a four-circle goniometer was possible. By means of multilayer shieldings (lead, brass, aluminium) the background count rate with the source mounted on the goniometer was reduced to 0·02 counts s^{-1}. The source area was 2·0 × 2·5 mm and the primary beam was collimated with a slit collimator made of pure aluminium (99·999%). The resulting divergence was 0·65° in the horizontal and 1·4° in the vertical direction. The counter aperture was 10 mm in diameter which corresponds to a divergence of 3·45°.

To separate the elastically scattered from the inelastically scattered radiation at least two measurements are necessary. One with the resonance conditions fulfilled, the other out of resonance. In most of the experiments described in the literature (Albanese *et al.*, 1972; Bärnighausen, 1975) the absorber is removed for the measurement out of resonance. The photoelectric absorption coefficient of the absorber has therefore to be determined separately. To avoid this additional uncertainty the goniometer was constructed in such a way that all measurements could be performed with the absorber fixed in front of the counter. Since the same area of the absorber was always illuminated the inhomogeneities of source and absorber (Ghezzi *et al.*, 1969) did not affect the measured intensities. This kind of measurement has the disadvantage that the source has to be moved with defined velocities and that the count rate for the measurement out of resonance is decreased but offers the possibility of increasing the accuracy.

For the source–absorber combination chosen in the present experiment, resonance condition is obtained with the source velocity set to zero. The experimental linewidth was determined in transmission geometry ($\Gamma = 0{\cdot}79$ mm s^{-1}). The measurements out of resonance were performed with $v = 3{\cdot}50$ mm s^{-1}, far away from the resonance conditions. As a further improvement of the standard experimental setup both a counter with high energy resolution (300 eV) and the necessary electronic equipment were selected, to allow an energy-dispersive mode of registration. In the selected energy window of 14·4 ± 0·4 keV for each angle (Fig. 2) a smooth energy dependence can be assumed for all radiation components contributing to the count rate (*e.g.* Compton scattering of the high-energy components of the source, cosmic and electronic background) with the only exception of the 14·4 keV ($\lambda = 0{\cdot}8602$ Å) Mössbauer radiation. The first contribution, in the following called background, was determined by performing linear regression on both sides of the energy window and a Hermite interpolation inside the window. After subtracting this contribution the remaining count rate could be fitted to a Gaussian distribution function and by integration the intensity for a selected source velocity, $I_v(\theta)$, was determined. For each measured angle the elastic fraction of the diffracted radiation is given by

$$p(\theta)=\frac{P(\theta)}{P(\theta=0)} \quad (1)$$

with

$$P(\theta)=\frac{I_v(\theta)-I_{v=0}(\theta)}{I_v(\theta)}. \quad (2)$$

$P(\theta=0)$ was determined in transmission geometry without a crystal, reducing the primary intensity I_0 by means of a collimator ($\varnothing=2{\cdot}0$ mm) situated in front of the counter. The integrated elastic intensity was therefore (Albanese *et al.*, 1972)

$$I_{el}(\theta)=p(\theta)I_v(\theta) \quad (3)$$

and the inelastic intensity

$$I_{inel}(\theta)=[1-p(\theta)]I_v(\theta). \quad (4)$$

To check the two selected source velocities ($v=0$ and $v=3{\cdot}5$ mm s^{-1}) and the goniometer setup with regard to mechanical stability, one of the reflections (400) was measured additionally with the source moved with constant acceleration. Data acquisition was performed at the same time with two different multichannel analysers, one switched in pulse-height-analysis mode (PHA), the other in multichannel-scaling mode (MCS). The PHA results were used for the background determination. From the MCS results P (equation 2) was determined. No energy shift or line broadening was observed for the scattered radiation compared with the results obtained in transmission geometry without a crystal. Linewidth and lineposition are therefore very accurate. For all investigated scattering angles the elastically scattered fraction $p(\theta)$ was in agreement for these two different measuring methods (Table 1). To save measuring time and to increase the accuracy all further experiments were performed only with the two constant source velocities $v=0{\cdot}00$ mm s^{-1} and $v=3{\cdot}50$ mm s^{-1}. Nevertheless, the time necessary to investigate one reflection was between 2 and 4 months.

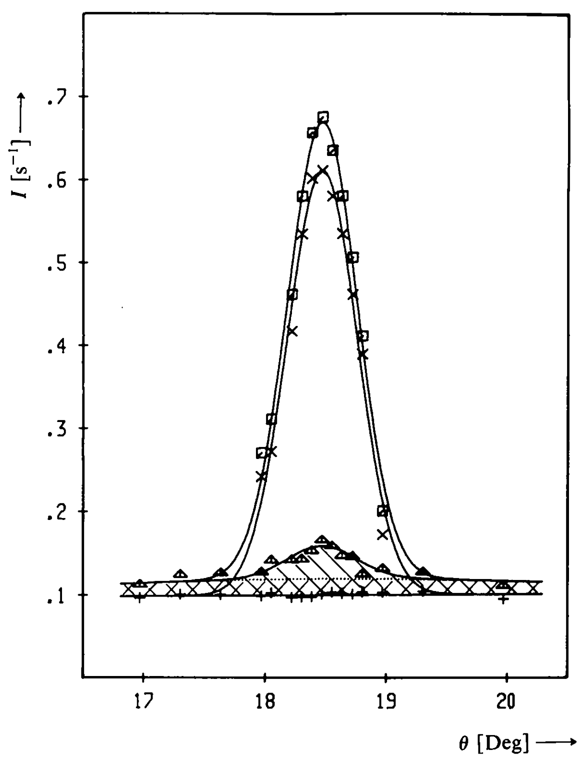

Fig. 2. Si 400 reflection. Inelastic (△), elastic (×) and total (□) intensity. Full curves calculated by means of Gaussian distribution functions. Background (+), full curve: linear regression. Hatched and cross-hatched area: total integrated TDS intensity. Cross-hatched area: integrated TDS intensity included in the background.

Table 1. *Comparison of the elastically scattered fraction p (θ) for the* 400 *reflection of* Si *for the two different measuring methods used*

Source moved with constant acceleration I, with constant velocities II.

θ (°)	p(θ) I	p(θ) II
17·97	0·79 (8)	0·79 (1)
18·30	0·91 (6)	0·898 (9)
18·47	0·91 (6)	0·888 (9)
18·64	0·92 (5)	0·916 (8)

A dislocation-free silicon single crystal, supplied by Wacker company (Burghausen), was cut perpendicular to the [100] axis. The overall dimensions of the plane parallel plate were $12\times10\times0{\cdot}2$ mm. Thus the illuminated area was always smaller than the crystal surface.

All measurements were performed at room temperature. The diffractometer was driven in a θ–2θ scan.

III. Results and discussion

Measurements in symmetric Bragg geometry were performed for the reflections 400, Fig. 2, and 800. In the angular range between these reflections the amount of inelastically scattered radiation was evaluated (Fig. 4). In addition the 511 reflection Fig. 3, was accessible in the same geometry.

A. Elastically scattered intensity

The lineshape of the angular dependence of the elastically scattered radiation was approximated by a Gaussian distribution function (Fig. 2). For all reflections the calculated width at half maximum was in complete agreement with that following from the divergence of the primary beam. The integrated scattered intensity was obtained by integration of the Gaussian function. To determine the temperature factor B a computer program was written by which the theoretical values for the integrated elastic intensities could be calculated from the dynamical theory (Batterman & Cole, 1964), taking into account the Prins correction by numerical integration. From the large number of atomic scattering factors reported in the literature those given in Table 2 were selected to calculate the structure factors. To correct these structure factors for dispersion the values given in *International Tables for X-ray Crystallography* (1968) were interpolated for the wavelength of the Mössbauer radiation. Using these corrected structure factors, B was varied until agreement was achieved between the measured and the calculated ratio of the integrated intensities of the 400 to the 800 reflection. In all calculations the linear absorption coefficient was set to 26·06 cm^{-1}. As an additional test the 511 reflection was investigated. The measured and calculated reflection coefficients are compared in Table 3 and are in very good agreement.

The value of B obtained by this fitting procedure is clearly dependent on the value of the atomic scattering factor. It is in very good agreement with the one given by Aldred & Hart (1973*a*, *b*) using the *Pendellösung* method (Table 2).

In spite of the good agreement with the *Pendellösung* method, the procedure of determining B from Mössbauer diffraction experiments has the disadvantage that for a further increase of the accuracy of the B value a larger number of reflections must be investigated, resulting in an unreasonable long measuring

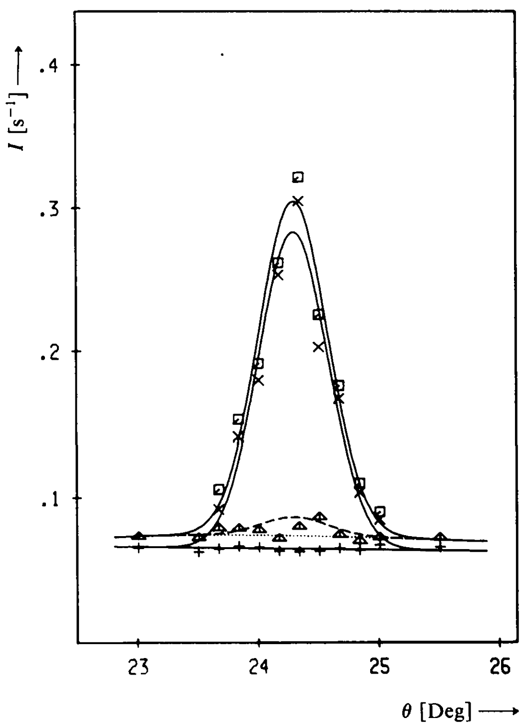

Fig. 3. Si 511 reflection. Symbols as described in Fig. 2. The broken line is only a guide for the eye.

Table 2. *Temperature factor B determined using different atomic scattering factors in comparison with literature* ($T = 295$ K)

References	B(Å²)
Aldred & Hart (1973*b*), exp.	0·4613 (27)
Graf, Schneider, Freund & Lehmann (1981), exp.	0·450 (11)
Fehlmann (1979), exp.	0·4515 (27)
Robertson & Reid (1979), theor.	0·5192
Present work	0·466 (41) ([a])
	0·422 (41) ([b])
	0·444 (41) ([c])
	0·436 (41) ([d])

Scattering factors taken from: (*a*) Aldred & Hart (1973*a*), exp.; (*b*) Yin & Cohen (1982), theor.; (*c*) Wang & Klein (1981), theor.; (*d*) *International Tables for X-ray Crystallography* (1974), theor.

Table 3. *Measured and calculated reflection coefficients* (I_{Bragg}/I_0) *using* $B = 0{\cdot}466$ Å^2

Reflection	Measured ($\times 10^{-6}$)	Calculated ($\times 10^{-6}$)
4 0 0	9·027 (4)	9·028
5 1 1	3·878 (5)	3·803
8 0 0	1·613 (1)	1·613

time due to the low activity of the currently available Mössbauer sources.

B. Inelastically scattered intensity

Corresponding to the high energy resolution of the Mössbauer effect, the part of the scattered radiation exhibiting an energy shift greater than 10 neV can be considered as inelastically scattered. In the whole angular range of the present investigation this inelastically scattered intensity was observable (Fig. 4), whereas an elastically scattered component was only detectable in the small angular range around the exact Bragg positions determined by the divergence of the primary beam. As described above, the background (Fig. 2) was always separated and the TDS intensity

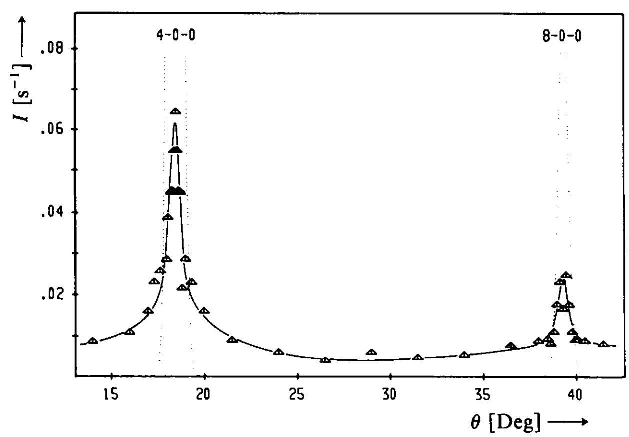

Fig. 4. Angular dependence of the inelastically scattered radiation of Si in the direction between the 400 and the 800 reflections. Symmetric Bragg case, θ–2θ scan. (Elastically scattered radiation · · ·.)

could be determined independently with an accuracy higher than the one reported in other Mössbauer diffraction experiments. The angular dependence of this inelastically scattered intensity in the angular range between the 400 and the 800 reflection is shown in Fig. 4. Since the inelastic intensity profile was in agreement with the TDS theory and the measurements were performed at room temperature it was assumed for the following that this intensity was caused by TDS only. However, this assumption will have to be verified by measurements at different temperatures.

A determination of the TDS intensity contributing to the measured total intensity of Bragg reflections is not possible in ordinary X-ray experiments due to the limited energy resolution. Therefore, it is necessary to estimate the TDS intensity by means of theoretical models. Most of these models are based on the long-wavelength approximation and are limited to first-order phonon scattering processes. Analytical methods to calculate the TDS contribution (Willis, 1969; Lucas, 1969) neglect the anisotropy of the elasticity and approximate the illuminated volume in reciprocal space either by a sphere or a cylinder. Different computer programs (Stevens, 1974; Kurittu & Merisalo, 1977; Helmoldt & Vos, 1977) are available which take into account an anisotropy of the elasticity and perform the integration in reciprocal space numerically. In addition, an estimation of the second-order TDS contribution is possible with the program of Stevens (1974). The elastic constants necessary for these calculations were taken from McSkimin & Andreatch (1964).

To compare the calculated results with the experiment for different scan lengths the total integrated TDS intensity was normalized to the measured integrated elastic intensity. This ratio was further converted from the dynamical to the kinematical approximation by using the theoretical extinction coefficient for a plane parallel plate of a perfect crystal and called I^{tot}_{TDS}/I_{Bragg} (Figs. 5, 6). The measured dependence of I^{tot}_{TDS}/I_{Bragg} on the scan length was in very good agreement with that calculated by means of the three computer programs, which were in complete agreement for the investigated angular interval. For scan lengths greater than 3·0° the observed deviation for the 800 reflection (Fig. 6) can be explained only partly by the neglect of higher-order phonon scattering contributions as indicated by the calculated second-order TDS dependence. Most of the observed deviation seems to be due to the limited applicability of the long-wavelength approximation, since for an illuminated volume of this size phonon wave vectors are essential for which the dispersion relation is no longer linear (Weber, 1977).

Robertson & Reid (1979) calculated the total phonon cross section for different reflections of silicon using the experimentally obtained B value of Aldred & Hart (1973*b*) for an illuminated volume of 1/4000 of the Brillouin zone. Taking into account the experimental geometry by the formula given by Reid (1973) good agreement was only obtained for a small interval of the scan length (Figs. 5, 6). This must mainly be due to the spherical approximation for the illuminated volume used in their calculations because a similar shape of the dependence of I^{tot}_{TDS}/I_{Bragg} on the scan length was obtained from the analytical model, where the same approximation of the illuminated volume was used. Taking a value of 6·427 km s^{-1} for the sound velocity in silicon, estimated after Willis & Pryor (1975) for both approximations of the illuminated volume, the TDS contribution is overestimated by the model of Willis for the 400 reflection (Fig. 5), whereas the TDS contribution is more precisely given for the 800 reflection, if the cylindrical approximation is used (Fig. 6).

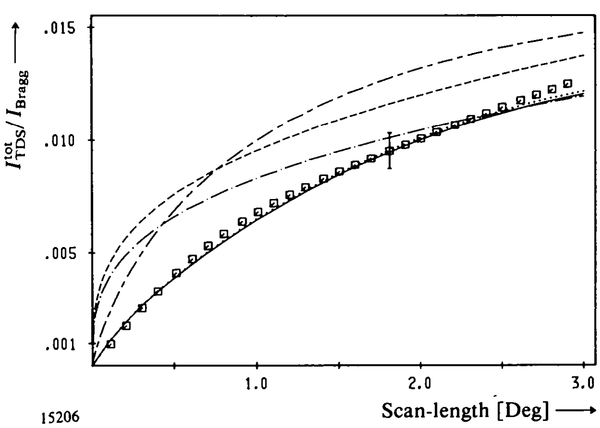

Fig. 5. Dependence of the ratio of the integrated total TDS intensity (I^{tot}_{TDS}) to the Bragg intensity (I_{Bragg}) on the scan length for the 400 reflection of Si. □ Measured; —— numerical calculations for first-order TDS after Stevens (1974), Helmholdt & Vos (1977) and Kurittu & Merisalo (1977); · · · · for first- and second-order TDS after Stevens (1974); analytical calculations (— — — spherical, - - - cylindrical approximation) after Willis & Pryor (1975) for first-order TDS, —·—· after Robertson & Reid (1979) (spherical approximation). For details see text.

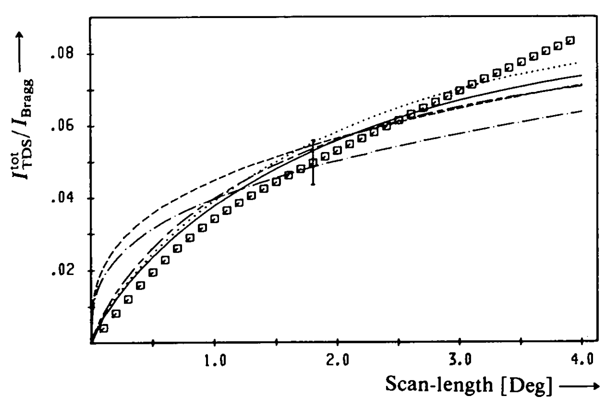

Fig. 6. I^{tot}_{TDS}/I_{Bragg} for the 800 reflection of Si. Symbols as described in Fig. 5.

Table 4. *TDS correction factor α for a chosen scan length of* 1·8°

		Calculated					
		Numerical			Analytical		
		St[a]	H & V[b]	K & M[c]	Lu[d]	W & P[e]	
Reflection	Measured					*s*	*c*
4 0 0	0·0042 (4)	0·0039	0·0039	0·0039	0·0061	0·0068	0·0075
8 0 0	0·021 (4)	0·0257	0·0252	0·0252	0·0247	0·0318	0·0281

Calculated after: (*a*) Stevens (1974); (*b*) Helmholdt & Vos (1977); (*c*) Kurittu & Merisalo (1977); (*d*) Lucas (1969); (*e*) Willis & Pryor (1975), *s* spherical approximation, *c* cylindrical approximation.

Following this comparison an estimation of the TDS intensity with high accuracy is possible by means of these different computer programs, if care is taken that for the experimental geometry the scan length is limited in such a way that the long-wavelength approximation is valid.

Since experimentally the background could be separated from the TDS contribution (Fig. 2), the TDS contribution to the background under the Bragg peak ($I^B_{\rm TDS}$) could be determined offering the possibility of measuring the TDS correction factor $\alpha = (I^{\rm tot}_{\rm TDS} - I^B_{\rm TDS})/I_{\rm Bragg}$. In Table 4 α is compared for a chosen scan length of 1·8° with the calculated correction factors using the above described methods. Whereas the values of α, calculated by the three computer programs agree with the measured ones, the values obtained from the analytical approximations given by Willis & Pryor (1975) and by Lucas (1969) overestimate the TDS contribution.

In addition, an attempt was made to determine the temperature factor B from the inelastic intensities to obtain further information about the analytical approximation of the TDS theory (Willis, 1969). From at least two reflections with parallel scattering vectors S, B can be evaluated, with the following assumptions: (i) the harmonic approximation is valid and (ii) the first-order TDS is the most dominant contribution. The integrated first-order TDS intensity is obtained from (Willis, 1969)

$$I_{\rm TDS} = \int\int \frac{{\rm d}\sigma(\mathbf{q})}{{\rm d}\Omega} {\rm d}\Theta\, {\rm d}\Omega \quad (5)$$

with the differential TDS cross section

$$\frac{{\rm d}\sigma(\mathbf{q})}{{\rm d}\Omega} \sim \frac{S^2}{q^2} |F_o(\mathbf{S})|^2 e^{-2BS^2} \times \sum_{j=1}^{3} \frac{E_j(\mathbf{q}) \cos^2 \beta_j(\mathbf{q})}{v_j^2} \quad (6)$$

(F_o structure factor for $B=0$, $\mathbf{q}$ phonon wave vector, $E_j(\mathbf{q})$ energy of mode j of $\mathbf{q}$, v_j velocity of mode j, β_j angle between S and mode j of $\mathbf{q}$). Since the direction of S was fixed $\beta_j(\mathbf{q})$ was constant. By calculating the ratio of the TDS intensities of the two reflections the summation over the polarization states was eliminated. The reciprocal space for the integration was approximated either by a sphere or a cylinder. The measured data were corrected for the influence of the second-order TDS by means of the program *TDS*2 (Stevens, 1974) and the TDS-background contributions were subtracted. Using the structure factors given by Aldred & Hart (1973*a*) from the ratio of the resulting integrated diffuse intensities of the 400 to the 800 reflections, $B = 0{\cdot}41\,(8)$ and $B = 0{\cdot}43\,(8)$ Å^2 were obtained for the spherical and cylindrical approximations of the illuminated volume, respectively. For both approximations for the illuminated volume, the B values are slightly smaller than those obtained from the elastically scattered radiation. This might be due to the simplifications which were involved in this analytical model (*e.g.* only one atom per unit cell, neglect of the anisotropy of the elasticity, approximations for the illuminated volume).

For the 511 reflection the shape of the TDS intensity under the Bragg peak (Fig. 3) is completely different to those obtained for both the 400 and 800 reflections. The observed behaviour can be explained by the presence of the 422 reciprocal-lattice point near to the surface of the Ewald sphere. For the scattering geometry used this lattice point can only influence the inelastically scattered intensity, but not that scattered elastically.

In summary, the diffraction of Mössbauer radiation can be used to perform measurements with such high accuracy that an experimental test of the predictions of lattice-dynamical models is possible.

The authors would like to thank Professor Tschirf, Ing. Schreiboeck and Mr Vogler for many helpful discussions and for the manufacture of the goniometer.

References

Albanese, G. & Deriu, A. (1979). *Riv. Nuovo Cimento*, **2**, 1–40.

Albanese, G., Ghezzi, C., Merlini, A. & Pace, S. (1972). *Phys. Rev. B*, **5**, 1746–1757.

Aldred, P. J. E. & Hart, M. (1973*a*). *Proc. R. Soc. London Ser. A*, **332**, 223–238.

Aldred, P. J. E. & Hart, M. (1973*b*). *Proc. R. Soc. London Ser. A*, **332**, 239–254.

Bärnighausen, E. (1975). *J. Appl. Cryst.* **8**, 477–487.

Batterman, B. W. & Cole, H. (1964). *Rev. Mod. Phys.* **36**, 681–717.

FEHLMANN, M. (1979). *J. Phys. Soc. Jpn*, **47**, 225–231.
GHEZZI, C., MERLINI, A. & PACE, S. (1969). *Nuovo Cimento*, **64**B, 103–115.
GRAF, H. A., SCHNEIDER, J. R., FREUND, A. K. & LEHMANN, M. S. (1981). *Acta Cryst.* **A37**, 863–871.
HELMHOLDT, R. B. & VOS, A. (1977). *Acta Cryst.* **A33**, 38–45.
International Tables for X-ray Crystallography (1968). Vol. III, edited by K. LONSDALE, pp. 213–217. Birmingham: Kynoch Press.
International Tables for X-ray Crystallography (1974). Vol. IV, edited by J. A. IBERS & W. C. HAMILTON, p. 99. Birmingham: Kynoch Press.
KASHIWASE, Y. & MINOURA, M. (1983). *Japn. J. Appl. Phys.* **22**, L49–L51.
KURITTU, J. & MERISALO, M. (1977). *Report Series in Physics*, No. 132, Univ. of Helsinki.
LUCAS, B. W. (1969). *Acta Cryst.* **A25**, 627–631.
MCSKIMIN, H. J. & ANDREATCH, P. (1964). *J. Appl. Phys.* **35**, 2161–2165.
O'CONNOR, D. A. & BUTT, N. M. (1963). *Phys. Lett.* **7**, 233–235.
REID, J. S. (1973). *Acta Cryst.* **A29**, 248–251.
REID, J. S. & PIRIE, J. D. (1980). *Acta Cryst.* **A36**, 957–965.
ROBERTSON, B. F. & REID, J. S. (1979). *Acta Cryst.* **A35**, 785–788.
STEVENS, E. D. (1974). *Acta Cryst.* **A30**, 184–189.
WANG, C. S. & KLEIN, B. M. (1981). *Phys. Rev. B*, **24**, 3393–3416.
WARREN, B. E. (1969). *X-ray Diffraction*, pp. 151–201. London: Addison Wesley.
WEBER, W. (1977). *Phys. Rev. B*, **15**, 4789–4803.
WILLIS, B. T. M. (1969). *Acta Cryst.* **A25**, 277–300.
WILLIS, B. T. M. & PRYOR, A. W. (1975). *Thermal Vibrations in Crystallography*, pp. 232–238. Cambridge Univ. Press.
YIN, M. T. & COHEN, M. L. (1982). *Phys. Rev. B*, **26**, 5668–5687.

Acta Cryst. (1984). A**40**, 465–468

Separation of Elastically and Inelastically Scattered γ-Radiation from $LiNbO_3$ by Mössbauer Diffraction

BY K. KREC, W. STEINER, P. PONGRATZ AND P. SKALICKY

Institut für Angewandte und Technische Physik, Technische Universität Wien, Austria

(*Received* 31 *January* 1983; *accepted* 22 *February* 1984)

Abstract

Mössbauer diffraction experiments have been performed on a $LiNbO_3$ single crystal at room temperature for scattering angles between 14·5 and 40·5°. A large contribution of inelastically scattered intensity was detectable for all scattering angles. Radiation damage caused by the high-energy components of the radiation emitted by the ^{57}Co Mössbauer source was observed. An attempt was made to estimate the temperature factor B from the measured inelastically scattered radiation assuming that first-order thermal diffuse scattering (TDS) is dominant. Both the TDS contribution to the integrated intensity within the Bragg peak and the ratio of the integrated first-order TDS included in the Bragg peak to that included in the background were calculated with various programs from the elastic constants and compared with the experimental values.

I. Introduction

Ferroelectrics like $LiNbO_3$ are of great interest for technical as well as scientific reasons. A comprehensive review of the properties of $LiNbO_3$ is given by Räuber (1978). Whereas extensive X-ray investigations (Abrahams, Reddy & Bernstein, 1966; Fujimoto, 1982), neutron scattering investigations (Chowdhury, Peckham & Saunderson, 1978) and some Mössbauer experiments on ^{57}Fe-doped crystals (Lauer, Pfannes & Keune, 1979; Pfannes, Lauer, Keune, Maeda & Sakai, 1980; Date, Gonser & Keune, 1979; Date, Joag, Engelmann, Keune & Gonser, 1981) have been reported, to our knowledge no measurements have been performed by means of Mössbauer diffraction. With this method the extraordinary high energy resolution of the Mössbauer effect can be used to measure both the elastically and the inelastically scattered radiation from crystals not containing Mössbauer isotopes. Therefore, it is possible to determine both the contribution of thermal diffuse scattering (TDS) to the intensities of Bragg reflections and the temperature factor B as demonstrated for a silicon single crystal (Krec & Steiner, 1984).

A direct determination of the temperature factor B from ordinary X-ray diffraction experiments is not possible (Lehmann, 1980). Abrahams *et al.* (1966) determined a mean value for B of 0.496 Å^2 from measurements of 247 reflections. Fujimoto (1982) obtained for a single crystal parallel to the hexagonal Z direction, the polar axis of $LiNbO_3$, a B value of 0·385 Å^2. Since these values are not in good agreement and also, an experimental proof of the applicability of TDS correction programs for such rather complicated structure types is desirable, Mössbauer diffraction experiments were performed on a single crystal of $LiNbO_3$ cut perpendicular to the piezoelectric Y axis to obtain additional information on the lattice dynamics.

In § II a short description of the experimental setup and the crystal orientation is given. The results for

0108-7673/84/040465-04$01.50